Microdomain Structures and Phase Transitions in Binary Blends Consisting of a Highly Asymmetric Block Copolymer and a Homopolymer

Nitin Y. Vaidya, Chang Dae Han,* and Do Kim

Department of Polymer Engineering, The University of Akron, Akron, Ohio 44325

Naoki Sakamoto and Takeji Hashimoto*

Department of Polymer Chemistry, Graduate School of Engineering, Kyoto University, Kyoto 606-8501, Japan

Received June 20, 2000; Revised Manuscript Received November 6, 2000

ABSTRACT: Microdomain structures and phase transitions in binary blends consisting of a highly asymmetric block copolymer and a homopolymer were investigated using transmission electron microscopy (TEM), small-angle X-ray scattering (SAXS), and oscillatory shear rheometry. For the study, a polystyrene-*block*-polyisoprene-*block*-polystyrene copolymer (Vector 4111) was mixed with a low molecular weight polystyrene (PS), where Vector 4111 has a 0.16 volume fraction of PS blocks. TEM images show that during heating from room temperature each of the binary blends prepared (86/14, 73/27, 62/38, and 49/51 Vector 4111/PS) exhibits "distorted microdomains" that have lost long-range order and yet have retained a distinct interface before reaching the micelle-free (or microdomain-free) homogeneous phase. SAXS measurements show that, during heating, each of the binary blends first undergoes lattice disordering transition and then demicellization transition. Following the terminologies introduced in our recent paper (*Macromolecules* **2000**, *33*, 3767), lattice disordering/ordering transition (LDOT) is a transition where ordered microdomains, during heating, transform into distorted microdimains (micelles without long-range order) and the micelles transform, during cooling, into ordered microdomains, and demicellization/micellization transition (DMT) is a transition where the micelles disappear, during heating, transforming into the micelle-free homogeneous state and micelles are formed, during cooling, from the micelle-free homogeneous phase. Analysis of SAXS results enabled us to determine the LDOT temperature (T_{LDOT}) and DMT temperature (T_{DMT}). It was found that the T_{DMT} determined by SAXS agreed well with those determined by oscillatory shear rheometry and that the addition of PS to Vector 4111 lowered the T_{DMT} of the block copolymer, the extent of which increased with increasing amounts of PS added. It is concluded that a simple rheological study is not sufficient in order to unambiguously determine different transitions in highly asymmetric block copolymer and its blends with a homopolymer and that it is imperative to combine rheological measurements with structural investigation.

Introduction

Today it is well established that the addition of a homopolymer to a block copolymer may bring about a change in microdomain structure in the block copolymer.[1−15] Under such situations, the entire amount of added homopolymer may reside within the microdomains of the block copolymer. Thus, some investigators[16−19] investigated the distributions of an added homopolymer within the microdomains of the block copolymer. However, depending upon the molecular weight of a homopolymer relative to the molecular weight of a block copolymer, the volume fraction of added homopolymer in the blend, and solubility limits that might exist between the homopolymer and the block copolymer, one encounters a situation where an excess amount of added homopolymer may induce macrophase separation, and thus the phase behavior of such a blend can indeed become very complex.[10,20−25] Experimental studies[10,20,21,23−25] report that the addition of a low molecular weight homopolymer to a block copolymer decreases its order−disorder transition (ODT) temperature (T_{ODT}).

A decrease in T_{ODT} of a block copolymer is highly desirable from the point of view of polymer processing, because the viscosity of a block copolymer decreases precipitously as the temperature crosses its T_{ODT},[26−28] thereby improving the processability of the block copolymer. It should be mentioned that most, if not all, of the commercially available diene-based triblock copolymers, often used for high-temperature melt adhesives, have T_{ODT} higher than the experimentally permissible temperature (say 220 °C) that can avoid thermal degradation and cross-linking reactions. Under such circumstances, one often adds a processing aid in order to lower the T_{ODT} of the block copolymer, so that the block copolymer can be processed at temperatures above its T_{ODT}.

In the past, theoretical studies[29−33] have been reported, predicting a decrease or an increase in T_{ODT} of block copolymer when a homopolymer is added. More recently, theoretical studies[32,33] have been reported on relating variations of microdomain structure with blend composition when a homopolymer A or B is added to an AB-type diblock copolymers.

To facilitate the discussion of our experimental results presented below, we have prepared a schematic, given in Figure 1, describing the disordering and ordering processes in a highly asymmetric neat block copolymer. With reference to Figure 1, during heating, a highly asymmetric block copolymer having body-centered-cubic (bcc) packing will first undergo lattice disordering transition and then demicellization transition. During cooling, a highly asymmetric block copolymer in the homogeneous state will first undergo micellization

10.1021/ma0010682 CCC: $20.00
Published on Web 12/15/2000

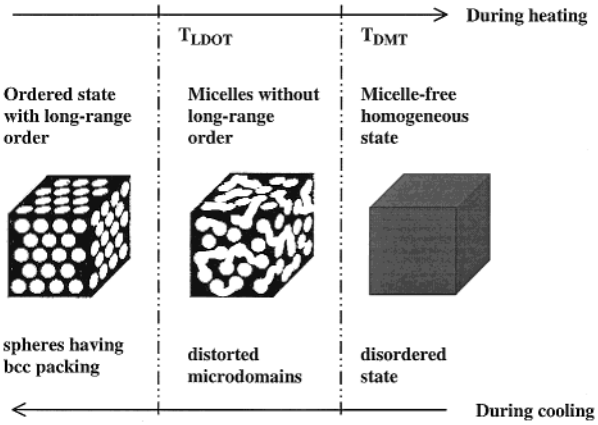

Figure 1. Schematic describing (i) the phase transitions' paths, during the heating process, from spheres with long-range order to distorted microdomains (micelles) without long-range order and to the micelle-free homogeneous state or (ii) the phase transitions' paths, during the cooling process, from the micelle-free homogeneous state to distorted microdomains without long-range order and to spheres with long-range order. In the schematic T_{LDOT} denotes "lattice disordering/ordering temperature" and T_{DMT} denotes "demicellization/micellization temperature". The demicellization/micellization transition may be called a "pseudo phase transition" in view of the fact that a finite number of molecules are involved in the transition.

transition and then lattice ordering transition. Following the terminologies introduced in our recent paper,[34] lattice disordering/ordering transition (LDOT) is a transition where ordered spherical microdomains in bcc lattice transform, during heating, into distorted microdomains (micelles without long-range order) and the micelles transform, during cooling, into ordered spherical microdomains. Also, demicellization/micellization transition (DMT) is a transition where the micelles disappear, during heating, transforming into the micelle-free homogeneous state and micelles are formed, during cooling, from the micelle-free homogeneous phase. That is, LDOT and DMT are thermally reversible transitions. With reference to Figure 1, T_{LDOT} denotes LDOT temperature and T_{DMT} denotes DMT temperature. In this paper we will elucidate that the same picture described above in conjunction with Figure 1 is also applicable to certain blends of block copolymer and homopolymer, and we will demonstrate the existence of LDOT and DMT as well as thermal reversibility in our blend system.[35]

As described in our previous paper,[34] DMT is not a true phase transition from a rigorous thermodynamic point of view, in the sense that it does not occur in effectively infinite systems, and hence it does not occur at a precise transition temperature with an infinite sharpness. Rather, DMT may be regarded as a pseudo-phase transition, involving effectively finite number of molecules and hence occurring over a finite range of temperatures.[36] The formation of micelles is an ordering process, and disappearance of micelles is a disordering process. It should be emphasized that the micelles are a thermodynamically stable phase, which will exist even at temperatures far above the T_g of the micelles and will not be destroyed in the temperature range between T_{LDOT} and T_{DMT}, by thermal energy, into composition fluctuations in the micelle-free homogeneous state.

On the other hand, for *symmetric* or *nearly symmetric* neat block copolymers, LDOT and DMT essentially degenerate into a single transition, ODT.[34] In other words, in symmetric or nearly symmetric block copolymers, microdomain structure with long-range order is transformed directly into the homogeneous phase at T_{ODT}, where the component blocks are mixed on a segmental level with some composition fluctuations.

From the point of view of the disordering of lattices in a block copolymer, the conventional definition of ODT and our definition of LDOT coincides (or are identical). However, a serious question may be raised as to whether there exists a structure at temperatures above T_{ODT} (T_{LDOT} in our definition). The answer to the question, on the basis of our previous study of neat block copolymers,[34] depends on the block copolymer composition; namely, highly asymmetric block copolymers possess a structure at temperatures above $T > T_{ODT}$ (T_{LDOT} in our definition), whereas symmetric or nearly symmetric block copolymers *do not*. We have found that such a structure, which is referred to as distorted microdomains (micelles),[34] is thermally stable, during heating, until reaching a critical temperature (T_{DMT} in our definition) at which the block copolymer begins to have a micelle-free homogeneous phase.[37] DMT may be regarded as an ordering process, just like the spinodal decomposition or the nucleation growth process in blends, except for a difference in length scale involved in the two systems; namely, DMT involves the case with the local scale having the sizes on the order of the radius of gyration (R_g) of sphere-forming block chains. When a structure exists at $T > T_{ODT}$ ($T > T_{LDOT}$ in our definition) in sphere-forming block copolymers, a distinction must be made between the two states: a state having distorted microdomains (micelles) at $T_{LDOT} \leq T < T_{DMT}$ and a state having micelle-free homogeneous phase at $T \geq T_{DMT}$. For the distinction, the terms LDOT and DMT will be very useful. If such a distinction is not made for highly asymmetric block copolymers, the morphological state of the block copolymers at $T > T_{ODT}$ will be left unclear. As a matter of fact, as early as 1983 Hashimoto and co-workers[39,40] first reported on the existence of two transition temperatures[41] in solutions consisting of a polystyrene-*block*-polybutadiene (SB diblock) copolymer and a selective solvent, *n*-tetradecane.

We must distinguish two situations where the formation of micelles in block copolymer may be observed. There is the situation where the formation of micelles may be observed when the concentration of a selective solvent added to a block copolymer is increased[39,40] or when the concentration of a low molecular weight homopolymer added to a block copolymer is increased.[5,6,25] Winey et al.[25] observed at room temperature, via SAXS and TEM, the formation of disordered micelles (DM according to their definition), upon increase in the concentration of homopolystyrene added to an SB diblock copolymer or to a polystyrene-*block*-polyisoprene (SI diblock) copolymer, from ordered microdomains although they did not report the onset of ODT (DMT in our terminology).[42] The micelle formation in a block copolymer/solvent system upon increasing temperature was studied only as a very special case by Hashimoto et al.,[40] who employed an SB diblock copolymer dissolved in a selective solvent, *n*-tetradecane. Note that *n*-tetradecane is a good solvent for polybutadiene (PB) chains but a poor solvent for polystyrene (PS) chains. They found that the added *n*-tetradecane swelled only the PB matrix phase, while the PS spherical microdomains were not swollen and kept vitrified or close to T_g even if not vitrified over the range of temperatures

where the PS spherical microdomains with long-range order transformed into micelles with increasing temperature.

There is another situation where the formation of micelles may be observed when a sphere-forming block copolymer is heated. In our previous study,[43] using small-angle X-ray scattering (SAXS), we found that a highly asymmetric polystyrene-*block*-polyisoprene-*block*-polystyrene (SIS triblock) copolymer (Vector 4111) with a 0.16 volume fraction of PS blocks (i) undergoes an order−order transition (OOT) at 179−185 °C with hexagonally packed cylindrical microdomains of PS at $T \leq 179$ °C, (ii) exhibits the coexistence of cylindrical and spherical microdomains of PS at 180 °C $\leq T \leq$ 185 °C, (iii) has spherical microdomains of PS in a cubic lattice at 185 °C $< T \leq$ 210 °C, and (iv) undergoes LDOT at temperatures between 210 °C (onset) and 214 °C (completion), and the spherical microdomain structure of PS with a liquidlike short-range order persists even up to 220 °C, the highest experimental temperature employed that could avoid thermal degradation and cross-linking reactions. Thus, we concluded that the T_{DMT} of Vector 4111 is much higher than 220 °C. In our most recent paper[34] we have reported on the microdomain structures and phase transitions in highly asymmetric polystyrene-*block*-polyisoprene (SI diblock) copolymers and that the transitions' paths, during heating, in a highly asymmetric SI block copolymer were quite different from the transition path involved in a nearly symmetric SI block copolymer.

Further, as will be presented below, the formation of micelles may be observed when a blend of highly asymmetric block copolymer and low molecular weight homopolymer is heated to a temperature above a critical temperature (T_{LDOT} in our terminology). Specifically, at low temperature the added homopolymer swells the PS spherical microdomains, which are then transformed into cylinders and to lamellae with long-range order as the amount of added homopolymer is increased. However, the ordered microphase, which is developed in the system containing a large volume fraction of the block copolymer, then is transformed, during heating, into distorted microdomains (micelles) at $T > T_{LDOT}$ and eventually into a micelle-free homogeneous phase at $T \geq T_{DMT}$. Therefore, the mechanism of micelle formation under such a circumstance is different from that observed in a block copolymer solution with increasing homopolymer or solvent concentration, where critical micelle concentration plays an important role. The temperature dependence of phase transition cannot easily be inferred from the concentration dependence of phase transition.

The present study was motivated in part by the desire to investigate, via SAXS and oscillatory shear rheometry, the extent to which the T_{DMT} of Vector 4111 can be lowered by the addition of a well-characterized low molecular weight homopolymer (PS-1). For the study we prepared binary blends consisting of Vector 4111 and PS-1. Also, using transmission electron microscopy (TEM), we investigated variations in the microdomain structures of Vector 4111/(PS-1) blends with increasing amounts of added PS-1 ranging from 14 to 51 wt %. We have found from TEM that at room temperature 86/14 and 73/27 Vector 4111/(PS-1) blends have hexagonally packed cylindrical microdomain structure and 62/38 and 49/51 Vector 4111/(PS-1) blends have lamellar microdomain structure. The results of the present study are quite different from the previous studies reported in the literature[1−15] in that during heating the Vector 4111/(PS-1) blends undergo first LDOT, transforming into distorted microdomains (micelles) at some intermediate temperatures, and then DMT at higher temperatures transforming into the micelle-free homogeneous phase, as determined by SAXS. The LDOT determined from SAXS was confirmed by TEM. Analysis of SAXS results enabled us to determine both T_{LDOT} and T_{DMT} of Vector 4111/(PS-1) blends. It was found that the T_{DMT} determined by SAXS agreed well with those determined by oscillatory shear rheometry. In this paper we show the consequences of neglecting the presence of distorted microdomains at $T > T_{LDOT}$ when constructing a phase diagram for Vector 4111/(PS-1) blends.

Table 1. Sample Code and Composition for the Vector 4111/(PS-1) Blends Investigated

sample code[a]	total wt fraction of PS
86/14 Vector 4111/(PS-1)	0.3
73/27 Vector 4111/(PS-1)	0.4
62/38 Vector 4111/(PS-1)	0.5
49/51 Vector 4111/(PS-1)	0.6

[a] The numbers refer to the weight percent (e.g., 86/14 Vector 4111/(PS-1) means 86 wt % Vector 4111 and 14 wt % PS-1).

Experimental Section

Materials and Sample Preparation. In preparing binary blends of a block copolymer and a homopolymer, we employed a commercially available, highly asymmetric SIS triblock copolymer (Vector 4111, Dexco Polymers Co.) having a number-average molecular weight (M_n) of 1.28×10^5 g/mol, a polydispersity index (M_w/M_n) of 1.11, and a 0.183 weight fraction of PS block determined by ^{1}H nuclear magnetic resonance spectroscopy. We also synthesized, via anionic polymerization, a low molecular weight polystyrene (PS-1) having $M_n = 1.0 \times 10^3$ g/mol and $M_w/M_n = 1.09$. The number-average molecular weight of each polymer was determined by membrane osmometry (Jupiter Instrument), and the polydispersity index was determined by gel permeation chromatography (Waters). Using these polymers, we prepared Vector 4111/(PS-1) binary blends by casting from a solution of the polymers with toluene. The choice of the Vector 4111/(PS-1) blends was motivated in part by the desire to bring down the T_{DMT} of Vector 4111, by the addition of PS-1, to the level of temperatures which would become experimentally accessible without being subjected to degradation and cross-linking reactions during experiment, because in our previous study we found that the T_{DMT} of Vector 4111 far exceeded 220 °C.[43]

Samples were prepared by first dissolving a predetermined amount of Vector 4111 and PS-1 in toluene (10 wt % in solution) in the presence of 0.1 wt % antioxidant (Irganox 1010, Ciba-Geigy Group) and then slowly evaporating the solvent. The evaporation of solvent was carried out initially in a fume hood slowly at room temperature for 1 week and then in a vacuum oven at 40 °C for 3 days for 86/14 and 73/27 Vector 4111/(PS-1) blends and for 5 days for 62/38 and 49/51 Vector 4111/(PS-1) blends, where the numbers refer to the weight percents. The last trace of solvent was removed by drying the samples in a vacuum oven at an elevated temperature by gradually raising the oven temperature from 40 to 110 °C for 86/14 and 73/27 Vector 4111/(PS-1) blends and from 40 to 60 °C for 62/38 and 49/51 Vector 4111/(PS-1) blends, at a rate of 10 °C/h. The drying of the samples was continued until there was no further change in weight and then annealed in a vacuum oven (i) at 130 °C for 10 h for 86/14 and 73/27 Vector 4111/(PS-1) blends, (ii) at 90 °C for 5 days for 62/38 Vector 4111/(PS-1) blend, and (iii) at 80 °C for 5 days for 49/51 Vector 4111/(PS-1) blend. These temperatures used for annealing are less than T_{LDOT} as will be clarified below. All specimens were quenched in ice water after thermal treatment and kept in the refrigerator before use in experiment. Table 1 gives a

summary of sample codes and compositions of the Vector 4111/(PS-1) binary blends.

Rheological Measurement. A Rheometrics mechanical spectrometer (model RMS 800) was employed in the oscillatory mode with parallel-plate fixture (25 mm diameter) (1) to conduct temperature sweep experiments in order to measure the dynamic storage modulus G' and dynamic loss modulus G'' at an angular frequency ω of 0.01 rad/s during heating and (2) to conduct frequency sweep experiments in order to measure G' and G'' as functions of ω ranging from 0.01 to 100 rad/s at various temperatures during heating. In conducting temperature sweep experiments under isochronal conditions, the specimen temperature was increased 2 °C/5 min stepwise. The frequency sweep experiment at a preset temperature lasted for about 45 min. The temperature control was accurate to within ±1 °C. In the rheological measurements a fixed strain of 0.04 was used at a given temperature, to ensure that measurements were taken well within the linear viscoelastic range of the materials investigated. All the rheological measurements were conducted under a nitrogen atmosphere in order to avoid oxidative degradation of the samples.

TEM Experiment. TEM was conducted to investigate the morphology of the neat block copolymers and their binary blends. The ultrathin sectioning was performed by cryoultramicrotomy at −100 °C, below the glass transition temperature ($T_g = -68$ °C) of polyisoprene (PI), to attain the rigidity of the specimen, using a Reichert Ultracut E low-temperature sectioning system. A transmission electron microscope (JEM1200EX II, JEOL) operated at 120 kV was used for taking pictures of the specimens stained with osmium tetroxide vapor. The annealing conditions employed for each specimen, before taking TEM, will be given below when we present TEM images.

SAXS Experiment. SAXS experiments were conducted under a nitrogen atmosphere, using an apparatus described in detail elsewhere[44,45] which consists of an 18 kW rotating-anode X-ray generator, a graphite crystal for incident-beam monochromatization, a 1.5 m camera, and a one-dimensional position-sensitive proportional counter (PSPC). The Cu Kα line ($\lambda = 0.154$ nm) was used. The SAXS profiles were measured stepwise every 5 or 10 °C for 30 min for the as-prepared samples of Vector 4111/(PS-1) in the heating and cooling processes with the waiting time of 15 min before each measurement. The SAXS profiles were corrected for absorption, air scattering, background scattering arising from thermal diffuse scattering, and slit-height and slit-width smearing.[46] The absolute SAXS intensity was obtained using the nickel-foil method.[47] The temperature control was accurate to within ±0.003 °C. The direction of the incident X-ray beam was perpendicular to the film surface of the specimens (referred to as "through view").

Results and Discussion

Microdomain Structures and Phase Transitions in Vector 4111/(PS-1) Blends. Figure 2 gives plots of log G' vs log G'' for the 86/14 Vector 4111/(PS-1) blend at various temperatures ranging from 140 to 220 °C, which were prepared from the dynamic frequency sweep experiments during heating. Following Neumann et al.,[48] below log G' vs log G'' plots will be referred to as Han plots. It is seen that Han plots having a slope of 2 in the terminal region start to be independent of temperature at 215 °C. Following the rheological criterion of Han et al.,[49] we conclude from Figure 2 that the T_{DMT} of this blend is approximately 215 °C. The parallel feature of Han plots in Figure 2, which represents liquidlike rheological behavior, originates from the presence of distorted microdomains with short-range spatial order.[34,43] Also given in the inset of Figure 2 is the temperature dependence of G' during the isochronal temperature sweep experiment at $\omega = 0.01$ rad/s in the heating process for the 86/14 Vector 4111/(PS-1) blend.

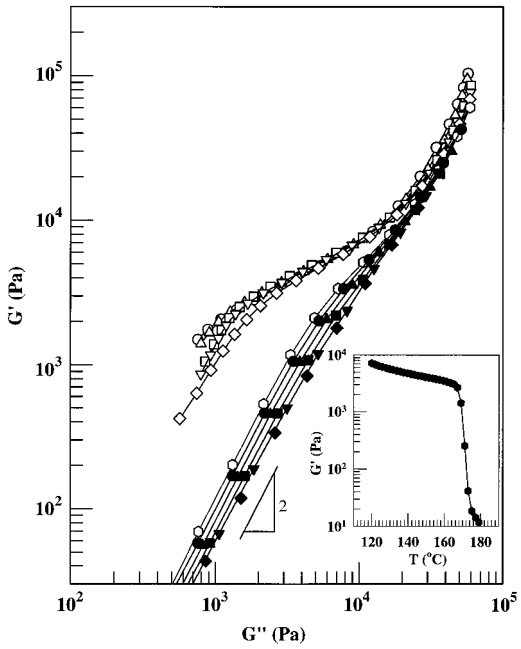

Figure 2. Han plots for the 86/14 Vector 4111/(PS-1) blend, in the heating process, at various temperatures: (○) 140, (△) 150, (□) 160, (▽) 165, (◇) 170, (⬡) 175, (●) 185, (▲) 195, (■) 205, (▼) 215, and (◆) 220 °C. For clarity, data points at 180, 190, 200, and 210 °C are not shown in this figure. The inset in the lower right corner gives the dependence of G' on temperature during the dynamic temperature sweep experiment under isochronal conditions at $\omega = 0.01$ rad/s in the heating process.

It can be seen in the inset that G' begins to drop precipitously at ca. 170 °C, which is far below the T_{DMT} (215 °C) determined from the Han plot. If we adopt the rheological criterion[50] that the temperature at which the value of G' drops abruptly in the log G' versus temperature plot represents T_{ODT} without checking via an independent experiment method whether there exists a structure at temperatures above T_{ODT}, one may conclude from Figure 2 that the T_{ODT} (T_{LDOT} in our terminology) of 86/14 Vector 4111/(PS-1) blend is approximately 170 °C, which is far below the T_{DMT} (215 °C) determined from the Han plot. Below, we will show from SAXS results that the 86/14 Vector 4111/(PS-1) blend indeed has a distorted microdomain structure at temperatures above 170 °C, and thus 170 °C represents the T_{LDOT}, but not the T_{ODT}, of the 86/14 Vector 4111/(PS-1) blend.

Figure 3 gives TEM images of the 86/14 Vector 4111/(PS-1) blend without and with annealing at various temperatures followed by quenching in ice water. The thermal histories of the specimens are given in the figure caption. In Figure 3 we observe that the 86/14 Vector 4111/(PS-1) blend has hexagonally packed cylinders at 25 °C, and hexagonally packed cylinders and distorted microdomain, which lost long-range order, coexist at 166 °C. It should be noted in Figure 3 that the long-range order of the microdomains disappears at 180 and 190 °C. The morphology at 180 and 190 °C exhibits distorted microdomains without long-range order, but we cannot determine precisely the morphology from this TEM image.

Figure 4 gives SAXS profiles for the 86/14 Vector 4111/(PS-1) blend at various temperatures ranging from 140 to 220 °C in the heating process. The intensities of the profiles shown at the top of the figure are actually

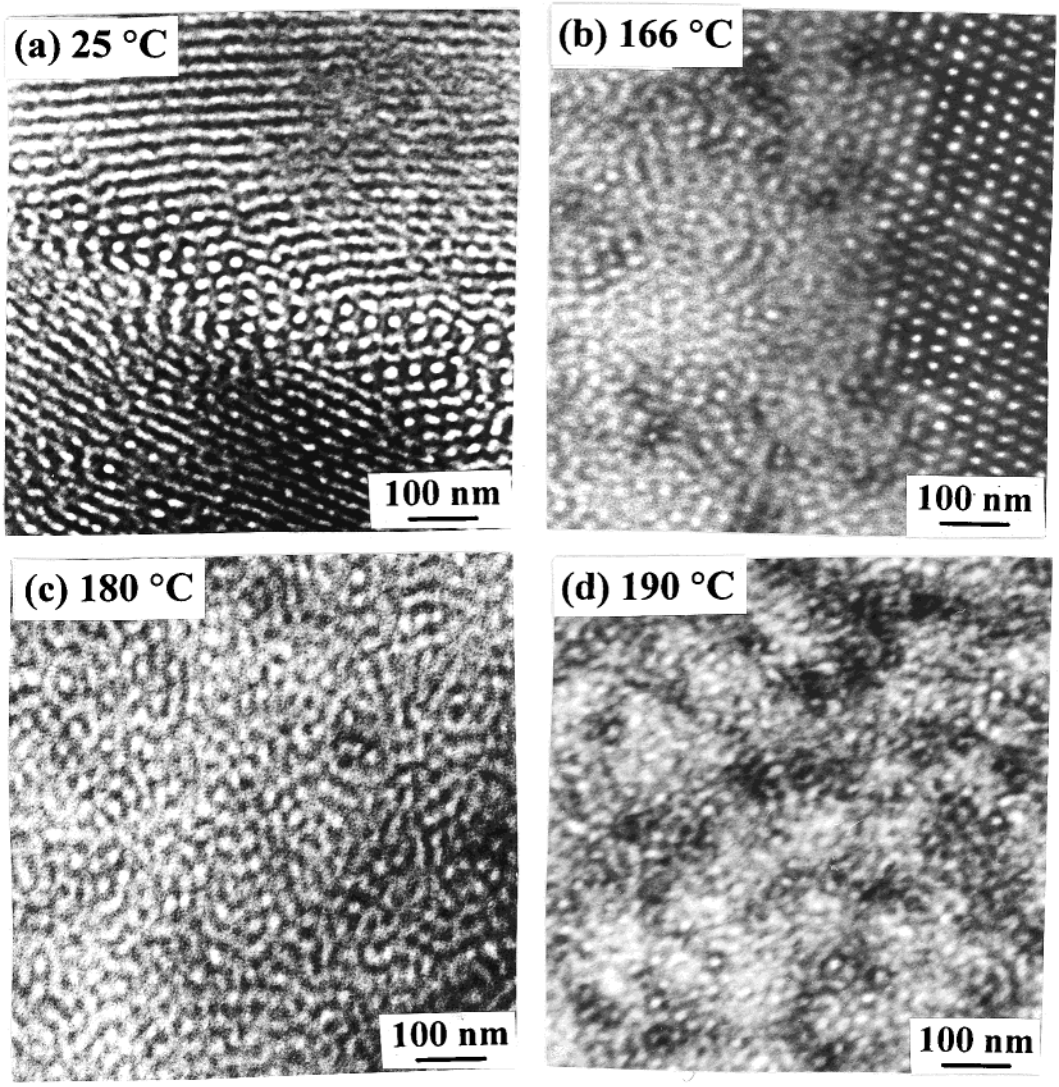

Figure 3. TEM images of the 86/14 Vector 4111/(PS-1) blend: (a) without annealing; (b) after annealing at 166 °C (below T_{LDOT}) for 10 h followed by quenching in ice water; (c) after annealing at 180 °C (above T_{LDOT} but below T_{DMT}) for 10 h followed by quenching in ice water; (d) after annealing at 190 °C for 10 h followed by quenching in ice water.

measured values, and in order to avoid overlaps, the intensities of the other profiles are shifted down by 1 decade relative to the SAXS intensities immediately above. The SAXS profile at 140 °C shows the higher order peaks at $q = \sqrt{3}q_m$ and $q = \sqrt{4}q_m$ with q_m being the wave vector q at the first-order scattering maximum, indicating that the morphology in the ordered state is the hexagonally packed cylinder. The intensity of the first-order peak decreases and the width of the first-order peak increases at temperatures between 165 and 175 °C, and both changes occur discontinuously, which can be seen more clearly and quantitatively in Figure 5. It suggests that the 86/14 Vector 4111/(PS-1) blend lost long-range order over this temperature interval. However, the shoulders at positions of $\sqrt{3}$ and $\sqrt{4}$ relative to q_m, which are overlapped into a single broad shoulder, exist even at 175 °C, indicating that domain or micelle structures still exist at this temperature. In addition, the asymptotic behavior of the scattering intensity distribution with respect to the magnitude of the scattering vector q in $0.25 < q < 0.6$ nm^{-1} has a slope of -4 at 175 °C, which is unaltered from that at 165 °C, implying that microdomains with a sharp interface exist at 175 °C. Thus, we conclude that LDOT takes place at temperatures between 165 and 175 °C; i.e., the hexagonal lattice disappears, but distorted microdomains with a short-range spatial order still exist above 175 °C. At 220 °C, only a single broad peak is observed, implying that the system is brought into the micelle-free disordered phase where the PS and PI block copolymer chains and PS-1 chains are mixed on a segmental level in a micelle-free disordered state.

With reference to Figure 4, we wish to mention that the lines with a slope of -4 are drawn somewhat arbitrarily in order to discuss the asymptotic behavior of the scattering intensity. We note, however, that the asymptotic behavior of $I(q)$ vs q in the double-logarithmic plot remains virtually unchanged below and above LDOT, while there are greater changes in the first-order and higher-order scattering maxima. This is a good indication that spheres exist as a structural entity below and above LDOT. We wish to point out that the asymptotic behavior of the scattering intensity with q changes below and above DMT. One might argue that the disappearance of higher-order SAXS peaks does not mean that a structure has gone. Such an argument may be valid, as a general statement, for scattering experiment of a dilute solution of micelles, for example. However, the polymer system being dealt with in this study is a melt consisting of block copolymer and

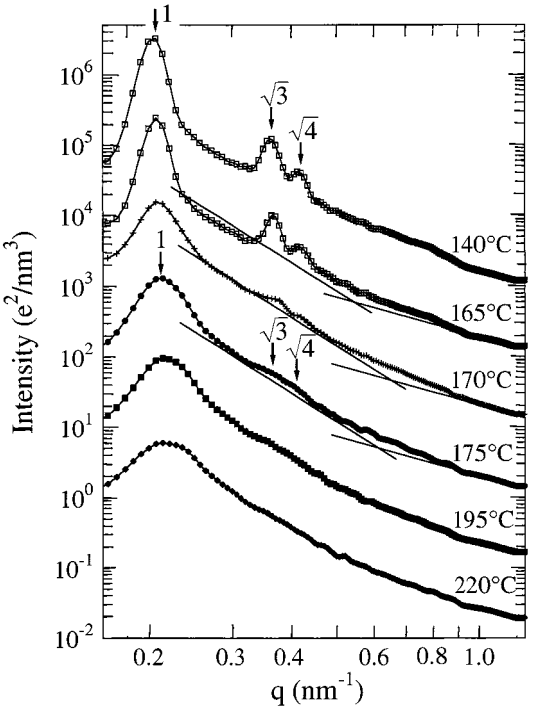

Figure 4. Temperature dependence of SAXS profiles for the 86/14 Vector 4111/(PS-1) blend in the heating process. The straight line having a slope of 4 is drawn to each SAXS profile to show the asymptotic behavior of $I(q) \sim q^{-4}$, while the straight line of slope −2 is drawn to each SAXS profile as a guide to the eye for the crossover behavior from q^{-4} to q^{-2}.

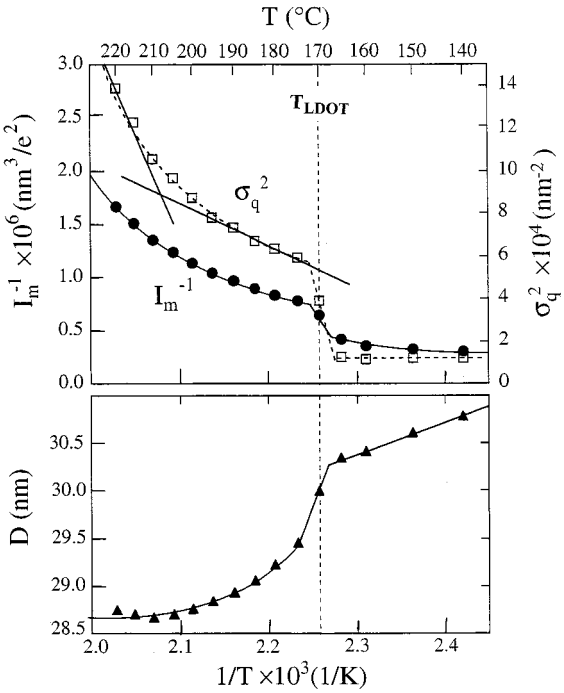

Figure 5. Plots of $1/I_m$ vs $1/T$, σ_q^2 vs $1/T$, and D vs $1/T$ for the 86/14 Vector 4111/(PS-1) blend from SAXS experiment in the heating process shown in Figure 4.

homopolystyrene, having the total weight fraction of PS ranging from 0.3 to 0.6 (see Table 1). Suppose that a structure exists in the 83/17 Vector 4111/(PS-1) blend after higher-order SAXS peaks disappeared. Such a structure must be smaller than ca. 5 nm in diameter that cannot be resolved by SAXS. It is well expected that such a structure cannot exist as a thermodynamically stable entity in our blend system. The disappearance of higher-order SAXS peaks or shoulders means, in our view, that the higher-order harmonics of Fourier component of composition fluctuations become negligibly small, implying that any structure units with clear interfaces have effectively gone.

Figure 5 gives plots of the reciprocal of the first-order peak intensity ($1/I_m$) vs the reciprocal of the absolute temperature ($1/T$), square of half-width at half-maximum (σ_q^2) of the first-order peak in SAXS profile vs $1/T$, and Bragg spacing ($D = 2\pi/q_m$) versus $1/T$ for the 86/14 Vector 4111/(PS-1) blend at temperatures ranging from 140 to 220 °C during the heating process. In Figure 5 we observe that a discontinuity in both $1/I_m$ and σ_q^2 starts at approximately 165 °C and completes at ca. 175 °C, and the temperature dependence of D also changes over the same temperature range. From the above observation we conclude that the T_{LDOT} of the Vector 4111/(PS-1) blend lies at temperatures between 165 and 175 °C. Above the T_{LDOT}, the system has distorted microdomains, and σ_q^2, $1/I_m$, and D change continuously with increasing temperature. We wish to mention that the LDOT in the 86/14 Vector 4111/(PS-1) blend observed by SAXS is thermally reversible as in the case of neat Vector 4111.[43]

As will be shown below and as found for Vector 4111,[43,51] all the systems undergoing LDOT do not exhibit a discontinuous change in σ_q^2 and $1/I_m$ at T_{DMT}, whereas the systems undergoing *no* LDOT exhibit a discontinuous change in σ_q^2 and $1/I_m$ at T_{ODT}.[52] This phenomenon can be interpreted as a consequence of degeneracy of two transitions, LDOT and DMT, into a single transition, ODT. Thus, the systems, such as Vector 4111/(PS-1) blends investigated in this study, appear to continuously change from distorted microdomains to the micelle-free homogeneous phase by increasing temperature above T_{LDOT}, which makes unequivocal determination of T_{DMT} for such systems difficult. In this study we tentatively determine T_{DMT} to be approximately 208 °C from the temperature at which the two straight lines drawn in Figure 5 intersect. Thus, we conclude from the SAXS results that 170 °C at which G' drops precipitously during the isochronal dynamic temperature sweep experiment (the inset of Figure 2) represents the T_{LDOT} and not T_{ODT} (T_{DMT} in our terminology) of the 86/14 Vector 4111/(PS-1) blend. We wish to mention that there is no rigorous theoretical basis for determination of T_{DMT} from the intersect of the two straight lines drawn in the plots of σ_q^2 vs $1/T$. However, from the basic principles of scattering, we can anticipate that the breadth of the scattering maximum arising from the distorted microdomains should be different from that arising from a micelle-free homogeneous melt. Similarly, the temperature dependence of σ_q^2 is expected to be different in the two regimes referred to above. At present, however, we do not have a firm theoretical basis supporting the method employed in this study to determine T_{DMT} from Figure 5.

We also have the results obtained from oscillatory rheometry, TEM, and SAXS for the 73/27 Vector 4111/(PS-1) blend. Owing to the space limitations here, those results are not presented here, and only the values of T_{LDOT} and T_{DMT} for the 73/27 Vector 4111/(PS-1) blend are summarized in Table 2.

Figure 6 gives Han plots for the 62/38 Vector 4111/(PS-1) blend at temperatures ranging from 80 to 170 °C in the heating process. It is seen that the Han plot

Table 2. Summary of T_{LDOT} and T_{DMT} for Vector 4111/(PS-1) Blends Determined in This Study

sample code[a]	T_{LDOT} (°C) from SAXS	T_{DMT} (°C) rheology	T_{DMT} (°C) SAXS
86/14 Vector 4111/(PS-1)	$165 < T_{LDOT} < 175$	215	208
73/27 Vector 4111/(PS-1)	$145 < T_{LDOT} < 155$	185	185
62/38 Vector 4111/(PS-1)	$130 < T_{LDOT} < 135$	160	155
49/51 Vector 4111/(PS-1)	$100 < T_{LDOT} < 110$	130	132

[a] The numbers refer to the weight percents.

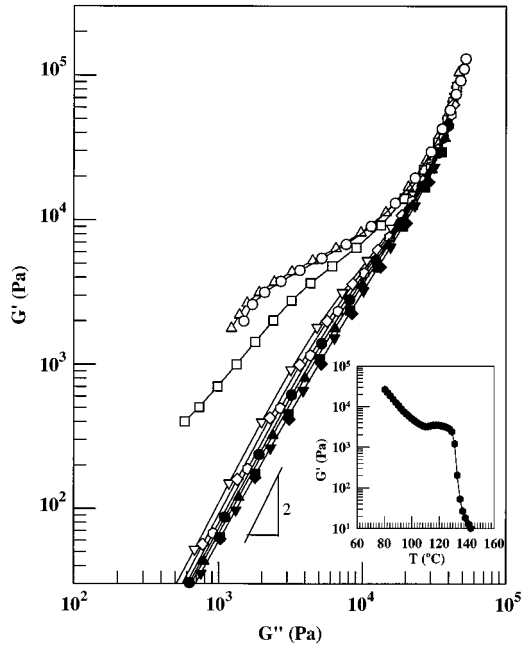

Figure 6. Han plots for the 62/38 Vector 4111/(PS-1) blend, in the heating process, at various temperatures: (○) 110, (△) 120, (□) 130, (▽) 135, (◇) 140, (⬡) 145, (●) 150, (▲) 155, (■) 160, (▼) 165, and (◆) 170 °C. For clarity, data points at 80, 90, 100, 105, 115, and 125 °C are not shown in this figure. The inset in the lower right corner gives the dependence of G' on temperature during the dynamic temperature sweep experiment under isochronal conditions at $\omega = 0.01$ rad/s in the heating process.

having a slope of 2 in the terminal region begins to be independent of temperature at 160 °C, from which we determine the T_{DMT} of this blend to be approximately 160 °C. The inset of Figure 6 gives the temperature dependence of G' during the isochronal temperature sweep experiment at $\omega = 0.01$ rad/s in the heating process for the 62/38 Vector 4111/(PS-1) blend, showing that a sudden drop in G' begins at approximately 130 °C, which is far below the T_{DMT} (160 °C) determined from the Han plot.

Figure 7 gives TEM images of the 62/38 Vector 4111/(PS-1) blend without and with annealing at various temperatures followed by quenching in ice water. The thermal histories of the specimens are given in the figure caption. In Figure 7 we observe that the 62/38 Vector 4111/(PS-1) blend has lamellar microdomains with sharp interface at 25 °C and distorted microdomains with a short-range spatial order at 120, 140, and 150 °C.

Figure 8 gives SAXS profiles for the 62/38 Vector 4111/(PS-1) blend at various temperatures ranging from 80 to 170 °C in the heating process. The second-order peak at $q = 2q_m$ at 80 °C indicates that the system forms lamellar microdomains with a long-range order at this temperature. An increase of added PS-1 from 14 to 38 wt % to Vector 4111 changed the morphology from the cylindrical to lamellar structure. However, in the SAXS profiles at 115 and 130 °C, the second-order peak exists at $q = \sqrt{3}q_m$, i.e., the ratio of the peak positions of the first- and second-order peaks changes from 1:2 to 1:$\sqrt{3}$ at temperatures between 80 and 115 °C, indicating that the OOT from lamellae to hexagonally packed cylinders takes place in this temperature interval. It is of interest to note that the first-order and higher-order peaks at 105 °C are much broader than those at 80 and 115 °C. It may reflect that the lamellar and cylindrical microdomains coexist at 105 °C; the SAXS profiles from lamellae and hexagonally packed cylinders have the maxima at the different positions in q value, and hence the peak width becomes broad when the scattering from lamellae and cylinders are superposed. The discontinuity in the peak intensity and the peak width are discerned at temperatures between 130 and 135 °C. However, the higher-order shoulder still exists at 135 °C, indicating that LDOT takes place (i.e., the hexagonal lattice disappears but the distorted microdomain still exists) in this temperature range.

Figure 9 gives plots of $1/I_m$ vs $1/T$, σ_q^2 vs $1/T$, and D vs $1/T$ for the 62/38 Vector 4111/(PS-1) blend at temperatures ranging from 80 to 170 °C during the heating process. In Figure 9 we observe that the $1/I_m$ and σ_q^2, especially σ_q^2, start to increase at 100 °C, reach a maximum value at 105 °C, and then decrease as the temperature is increased to 115 °C, indicating that the OOT starts at 100 °C and completes at 115 °C. In this temperature interval the temperature dependence of D also changes. With further increasing temperature, both $1/I_m$ and σ_q^2 increase discontinuously at temperatures between 130 and 135 °C, and the temperature dependence of D also changes in the same temperature range. The above observation suggests to us that the 62/38 Vector 4111/(PS-1) blend undergoes OOT at temperatures between 100 and 115 °C and LDOT at temperatures between 130 and 135 °C. We determine the T_{DMT} of the 62/38 Vector 4111/(PS-1) blend to be approximately 155 °C from the intersection of the two solid lines in the plot of σ_q^2 vs $1/T$ in Figure 9. Thus, we conclude that 130 °C at which G' drops precipitously during the isochronal dynamic temperature sweep experiment (the inset of Figure 6) represents the T_{LDOT} of the 62/38 Vector 4111/(PS-1) blend. Although OOT itself for this blend is an interesting phenomenon, further discussion of this subject is beyond the scope of this paper.

Figure 10 gives Han plots for the 49/51 Vector 4111/(PS-1) blend at temperatures ranging from 80 to 140 °C in the heating process. It is seen that the Han plot having a slope of 2 in the terminal region begins to be independent of temperature at 130 °C, from which we determine the T_{DMT} of this blend to be approximately 130 °C.

Figure 11 gives SAXS profiles for 49/51 Vector 4111/(PS-1) blend at various temperatures ranging from 90 to 140 °C in the heating cycle. The higher-order peak exists at $q = 2q_m$ at 90 and 100 °C, indicating that this blend has lamellar microdomains in the ordered state. The peak broadening at temperatures between 100 and 110 °C suggests that LDOT takes place in this temperature range. Figure 12 gives plots of $1/I_m$ vs $1/T$, σ_q^2 vs $1/T$, and D vs $1/T$ for 49/51 Vector 4111/(PS-1) blend at temperatures ranging from 80 to 140 °C during the heating cycle. In Figure 12 we observe that the discontinuity in both $1/I_m$ and σ_q^2 starts at approximately 100

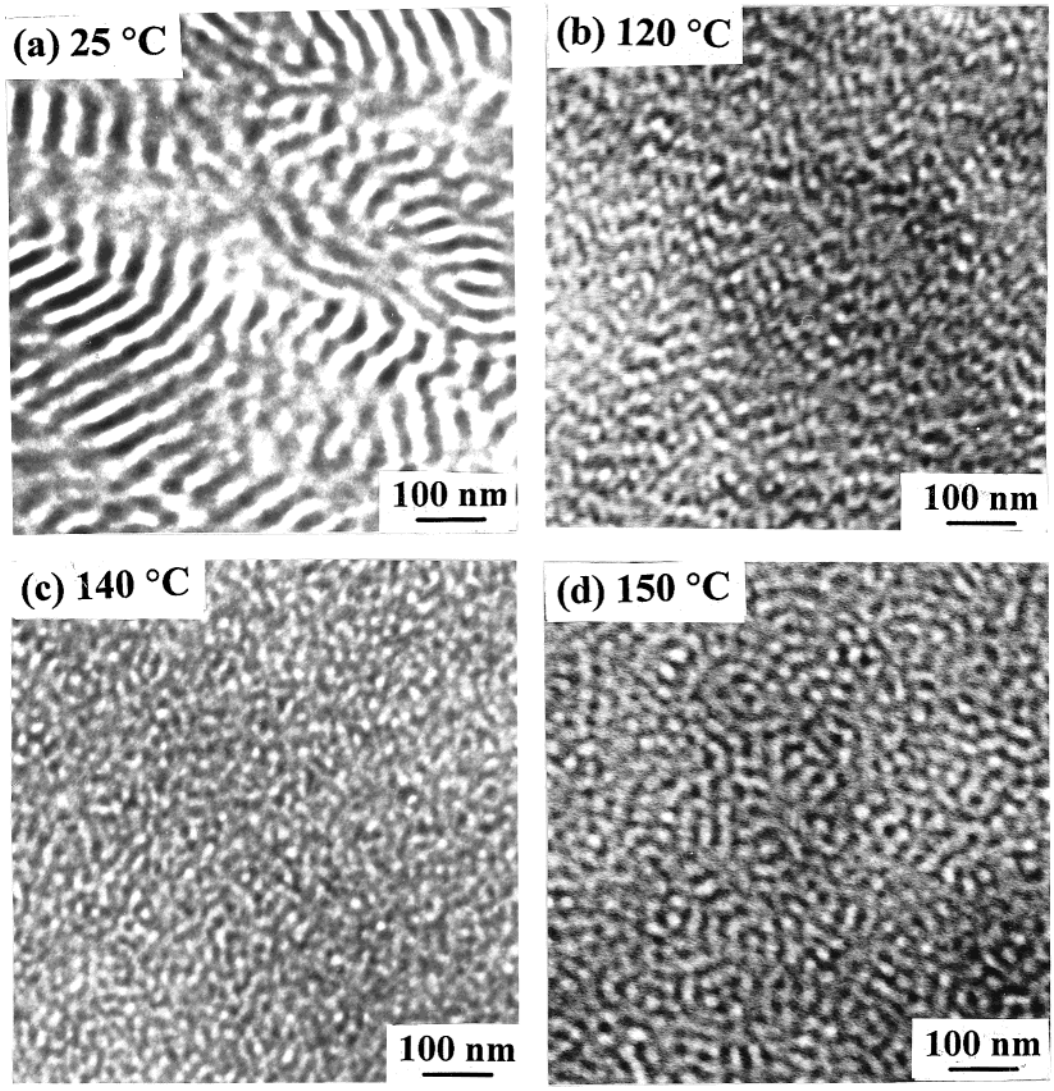

Figure 7. TEM images of the 62/38 Vector 4111/(PS-1) blend: (a) without annealing; (b) after annealing at 120 °C (below T_{LDOT}) for 1 day followed by quenching in ice water; (c) after annealing at 140 °C for 3 days followed by quenching in ice water; (d) after annealing at 150 °C (above T_{LDOT} but below T_{DMT}) for 10 h followed by quenching in ice water.

°C and completes at approximately 110 °C, and the temperature dependence of D, dD/d(1/T), also changes, though small, over the same temperature range. From the above observation we conclude that the T_{LDOT} of 49/51 Vector 4111/(PS-1) blend lies at temperatures between 100 and 110 °C. From the intersection of the two solid lines in the plot of σ_q^2 vs 1/T in Figure 12, we determine the T_{DMT} of 49/51 Vector 4111/(PS-1) blend to be approximately 132 °C.[53] Thus, for this blend with a high content of PS-1 we cannot discern OOT, in contrast with the 62/38 Vector 4111/(PS-1) blend shown in Figure 9. This is probably due to the fact that LDOT occurred prior to OOT in the 49/51 Vector 4111/(PS-1) blend having a high content of PS-1.

The SAXS profiles for 49/51 Vector 4111/(PS-1) blend obtained in the *cooling* cycle were found to be very similar to those in Figure 11, though not presented here, namely, the SAXS profiles at temperatures above 110 °C have a broad first-order peak, while those below 100 °C have sharp first-order and second-order peaks at $q = 2q_m$. Figure 13 gives plots of $1/I_m$ vs 1/T and σ_q^2 vs 1/T for 49/51 Vector 4111/(PS-1) blend at temperatures ranging from 135 to 80 °C during the cooling cycle. The temperature protocol employed for the cooling experiment is as follows: the temperature of a specimen was decreased stepwise from 135 °C in the homogeneous state to 80 °C following a predetermined temperature interval. Fifteen minutes was allowed for attaining thermal equilibrium before SAXS measurement began, and the SAXS measurement at each temperature lasted for 30 min for each temperature. In Figure 13 we observe a discontinuity in both $1/I_m$ and σ_q^2 at temperatures between 100 and 110 °C. This feature indicates that the lattice ordering into the alternating layers of lamellar assembly occurs at the same temperature interval as that of the LDOT in the heating cycle; i.e., there is no hysteresis in the thermally reversible lattice disordering and lattice ordering transitions, provided that the rate of temperature change is sufficiently slow compared to the rate of ordering and disordering.

It should be mentioned at this juncture that (1) the specimens used in the present study were transparent, (2) the intensity of the SAXS at values of q very close to zero ($q \approx 0$) did not increase with the addition of PS-1, and (3) a large bright area corresponding to the macrophase-separated PS-1 was not observed in the TEM images. Such evidence suggests that macrophase separation did not occur in all four Vector 4111/(PS-1) blends investigated in this study over the entire range

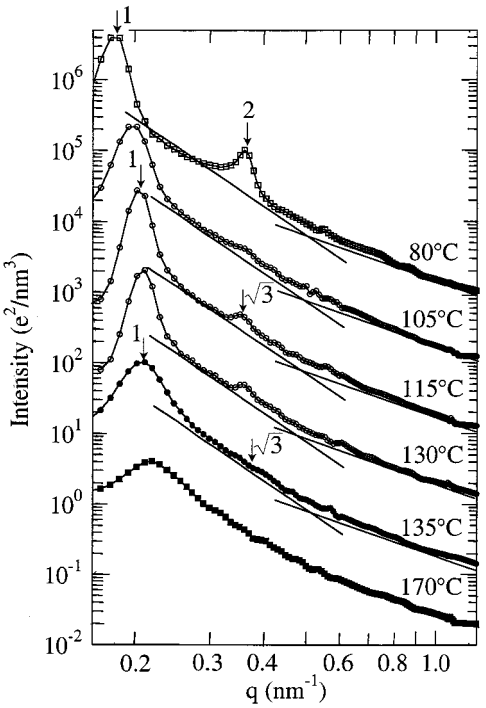

Figure 8. Temperature dependence of SAXS profiles for the 62/38 Vector 4111/(PS-1) blend in the heating process. The straight line having a slope of 4 is drawn to each SAXS profile to show the asymptotic behavior of $I(q) \sim q^{-4}$, while the straight line of slope −2 is drawn to each SAXS profile as a guide to the eye for the crossover behavior from q^{-4} to q^{-2}.

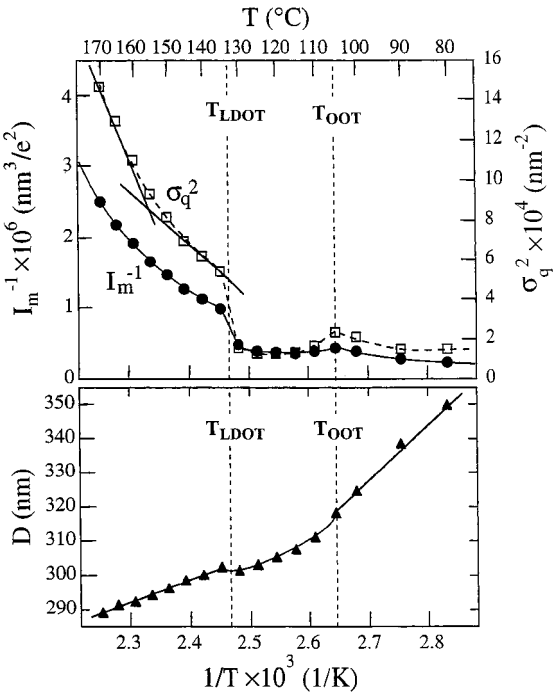

Figure 9. Plots of $1/I_m$ vs $1/T$, σ_q^2 vs $1/T$, and D vs $1/T$ for the 62/38 Vector 4111/(PS-1) blend from SAXS experiment in the heating process shown in Figure 8.

of temperatures at which SAXS measurements were taken.

Origin of the Parallel Feature of Han Plot in the Terminal Region. In the rheological results presented above (Figures 2, 6, and 10), we have observed LDOT taking place in the Vector 4111/(PS-1) blends before transforming into the micelle-free homogeneous state. Note that both TEM images (Figures 3 and 7) and SAXS

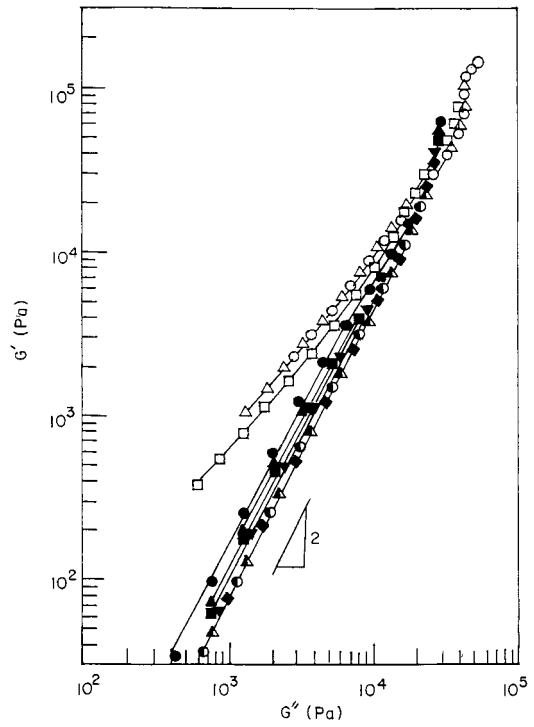

Figure 10. Han plots for the 49/51 Vector 4111/(PS-1) blend during heating at various temperatures: (○) 80, (△) 90, (□) 100, (●) 110, (▲) 115, (■) 120, (▼) 125, (◆) 130, (◐) 135, and (◭) 140 °C.

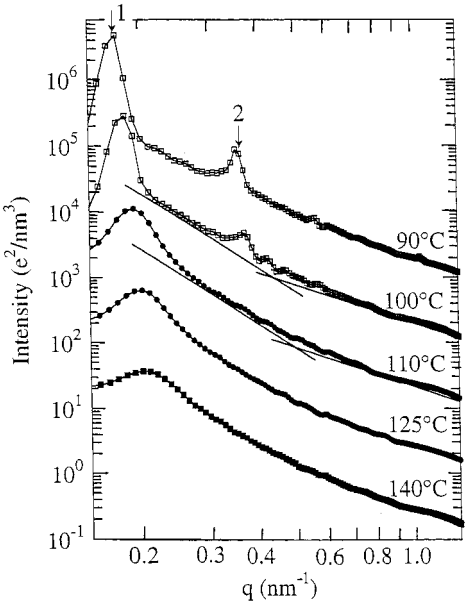

Figure 11. Temperature dependence of SAXS profiles for the 49/51 Vector 4111/(PS-1) blend during heating. The straight line having a slope of 4 is drawn to each SAXS profile to show the asymptotic behavior of $I(q) \sim q^{-4}$, while the straight line of slope −2 is drawn to each SAXS profile as a guide to the eye for the crossover behavior from q^{-4} to q^{-2}.

results (Figures 4, 5, 8, 9, and 11−13) show clearly that at $T_{LDOT} < T < T_{DMT}$ each of the Vector 4111/(PS-1) blends has distorted microdomains with short-range spatial order although the Han plots in the terminal region have a slope of 2 in this temperature region. The origin of the liquidlike rheological behavior observed in the terminal region of the Han plot (Figures 2, 6, and 10) at $T_{LDOT} < T < T_{DMT}$ lies in that (i) in the terminal region the micelles as a whole can flow, giving rise to

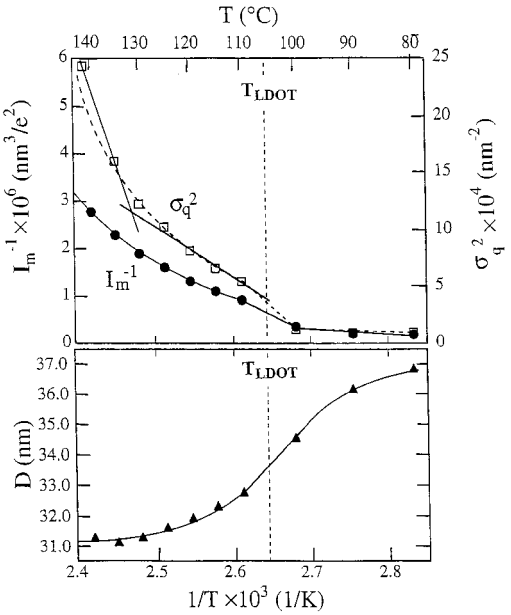

Figure 12. Plots of $1/I_m$ vs $1/T$, σ_q^2 vs $1/T$, and D vs $1/T$ for the 49/51 Vector 4111/(PS-1) blend from SAXS experiment during heating.

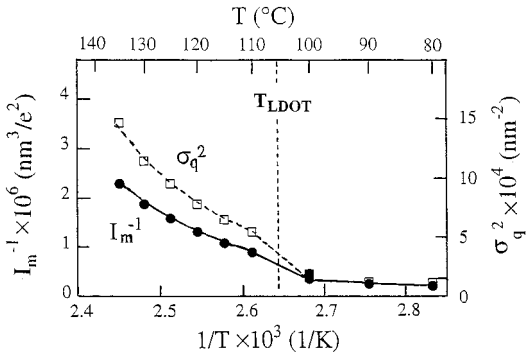

Figure 13. Plots of $1/I_m$ vs $1/T$ and σ_q^2 vs $1/T$ for the 49/51 Vector 4111/(PS-1) blend from SAXS experiment during cooling.

liquidlike rheological response (e.g., $G' \propto \omega^2$ and $G'' \propto \omega$), and (ii) as T_{DMT} is approached, the modulus of micelles decreases, giving rise to the parallel feature with a downward shift in the Han plot (mechanical origin of the shift). It should also be noted that as T_{DMT} is approached, the segregation power between the PS and PI block chains decreases, and hence PS chains in the PS domains can be more easily pulled out from the domains into the matrix, allowing the system to flow more easily (thermodynamic origin of the shift).

The factor responsible for causing LDOT in highly asymmetric block copolymers (Vector 4111) and their blends with a low molecular-weight PS investigated in this study is a difference in thermal stability between the lattice itself and the micelles themselves on the lattice.[38] As the temperature is raised, random thermal forces increase. Even under this situation the micelles themselves can maintain thermodynamic stability, driven by the segregation power between the PS and PI block chains, against random thermal forces at temperatures below T_{DMT}. However, the lattice itself may lose thermal stability at T_{LDOT}, much lower than T_{DMT}, due to increased conformational fluctuations of block chains driven by the increased random thermal force. At high temperatures (say at $T > T_{g,PS} + 60$ °C) the low molecular weight PS-1 chains have a low viscosity and exhibit liquidlike behavior. As a result, they effectively enhance the random thermal forces, causing enhanced conformational fluctuations of block chains and composition fluctuations of homopolymers. The enhanced random thermal forces destroy the packing order and give rise to a lattice-disordered state at T_{LDOT} before transforming into the micelle-free homogeneous phase upon further increase in temperature.

LDOT in Highly Asymmetric Block Copolymer/Homopolymer Blends. In our previous paper[43] we reported experimental observations, via TEM and SAXS, of LDOT in Vector 4111. In that paper, we made a distinction between LDT and ODT (LDOT and DMT in the terminology defined in Figure 1). Although LDOT and DMT degenerate into ODT within the spirit of the mean-field theory of Leibler,[55] we emphasize here that in the Vector 4111/(PS-1) blends the microdomains with a long-range order is transformed into distorted microdomains (micelles) with a short-range liquidlike order at and above the T_{LDOT}. As the temperature is increased further, eventually the distorted microdomains are transformed into the micelle-free homogeneous phase, in which only thermally induced composition fluctuations may exist upon raising the temperature above T_{DMT}.

The presence of distorted microdomains was manifested by the following pieces of evidence from SAXS study: (i) the higher-order shoulder exists in the SAXS profile at temperatures even above the T_{LDOT} and below the T_{DMT}, (ii) the asymptotic behavior of the SAXS scattering intensity distribution with respect to the magnitude of the scattering vector q in a high-q region is unaltered across the T_{LDOT}, and (iii) the remarkable change in $d(\sigma_q^2)/d(1/T)$ below and above T_{DMT}. Thus, we must distinguish the LDOT and DMT in the present study dealing with highly asymmetric diblock copolymers and their blends with low molecular weight PS. In the previous paper,[43] we stressed our view that the disordered spheres with short-range liquidlike order in Vector 4111 was generated by the random thermal forces, which perturbed the long-range order of spheres in bcc lattice. It should be noted that the effect of random thermal force on the bcc spheres is neglected in Leibler's theory.[55] On the other hand, the random thermal force plays important role in highly asymmetric block copolymers and their blends with a homopolymer.

In the present study we observed, via SAXS, that LDOT takes place in Vector 4111/(PS-1) blends (Figures 4, 5, 8, 9, and 11−13). We have shown that the LDOT is thermally reversible (see, for example, Figure 13). In addition, the addition of PS-1 to Vector 4111 enabled us to observe DMT in the Vector 4111/(PS-1) blends investigated. Table 2 gives a summary of the T_{LDOT}'s and T_{DMT}'s for the Vector 4111/(PS-1) blends determined from SAXS, and they are compared with the values obtained from the Han plot. We find that both T_{LDOT} and T_{DMT} decrease with increasing amount of low molecular weight homopolymer PS. The results of the present study on Vector 4111/(PS-1) blends are quite different from those of our previous study[43] on Vector 4111 in that in the present study LDOT takes place regardless of whether the microdomains of the Vector 4111/(PS-1) blends just below T_{LDOT} were lamellae, hexagonally packed cylinders, or spheres in bcc lattice, whereas in the previous study the microdomains of Vector 4111 just below T_{LDOT} were spheres in a bcc lattice. To the best of our knowledge, all the recent

studies on neat block copolymers having lamellar or hexagonally packed cylindrical microdomains show that an ordered state with long-range order is directly transformed into the homogeneous state upon raising the temperature above T_{ODT}; i.e., the ODT and LDOT are degenerated.

At this juncture it is worth mentioning that very recently Bodycomb et al.[56] conducted in-situ SAXS experiments to investigate the phase behavior of binary blends consisting of a *nearly symmetric* SI diblock copolymer (SI-11/9) and a low molecular weight homopolystyrene (S-6), where SI-11/9 has a molecular weight of 2.0×10^4 and a 0.51 volume fraction of PS block, and S-6 has a molecular weight of 6.1×10^3. They observed the existence of DMT in 0.44/0.56 and 0.36/0.64 (SI-11/9)/(S-6) blends exhibiting disordered spheres at low temperatures, where 0.44/0.56 and 0.36/0.64 refer to the volume fraction of the component polymers, while the blends with higher volume fractions of block copolymer, exhibiting lamellae, gyroid, and cylinders with long-range order, underwent ODT only, as found in neat lamella- or cylinder-forming block copolymers.[57] Their study indicates that the existence of DMT is not restricted only to binary blends consisting of a highly asymmetric block copolymer and a homopolymer, the results of which are summarized in this paper.

It seems appropriate to mention at this juncture that in our previous study[51] we also observed, via SAXS, LDOT taking place when a neutral solvent, dioctyl phthalate (DOP), was added to Vector 4111. In that study, we observed that the microdomains of a 85.5/14.5 Vector 4111/DOP blend just below T_{LDOT} were spheres in a cubic lattice. This can be easily understood from the point of view that DOP is a neutral solvent for both PS and PI blocks of Vector 4111, thus simply playing the role of a diluent and not affecting the morphology of Vector 4111. On the other hand, in the present study the added PS-1 is selectively solubilized into the PS cylinders of Vector 4111, giving rise to a morphological transformation depending upon the amount of PS-1 added.

The observation made above from SAXS, showing that LDOT takes place, is supported further by TEM. Specifically, the TEM images show that the morphology at $T_{LDOT} < T < T_{DMT}$ is virtually the same in 86/14 Vector 4111/(PS-1) blend investigated in this study; i.e., it is a distorted microdomain with a short-range spatial order although the morphology just below T_{LDOT} was different for different blends. The morphology in the distorted microdomains should be identified as a function of homopolymer composition in future investigation.

Concluding Remarks

One of the motivations of the present study was to determine, or at least to estimate, the T_{DMT} of Vector 4111 by adding a low molecular weight polystyrene, PS-1, because in our previous study[43] we could not determine the T_{DMT} of Vector 4111 during heating to 220 °C, the highest experimental temperature employed without a possibility of having cross-linking and degradation reactions.

In the present study we have found that the temperature at which G' decreased precipitously during the isochronal dynamic temperature sweep experiment (Figures 2 and 6) corresponds to T_{LDOT}, but not the T_{DMT}, when compared with SAXS results (Figures 4, 5, 8, and 9). Such an observation leads us to conclude that the isochronal dynamic temperature sweep experiment is not useful to determine the T_{DMT}'s of binary blends consisting of a highly asymmetric block copolymer and a low molecular weight homopolymer. We have found the values of T_{DMT} determined from Han plots agree reasonably well with those determined by SAXS (Table 2).

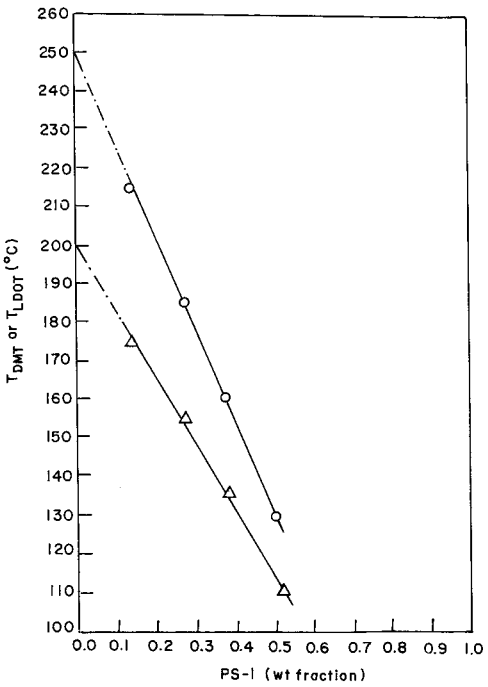

Figure 14. Effect of addition of PS-1 on the T_{DMT} and T_{LDOT} of Vector 4111/(PS-1) blends: (○) T_{DMT} and (△) T_{LDOT}.

We have found that addition of PS-1 decreased the T_{DMT} of Vector 4111. Figure 14 describes the effect of addition of PS-1 on the T_{MDT} and T_{LDOT} of Vector 4111/(PS-1) blends. It is seen that both T_{MDT} and T_{LDOT} decrease monotonically with increasing the amount of added PS-1. If an extrapolation, as shown by the broken line in Figure 14, of the measured T_{DMT} and T_{LDOT} of the Vector 4111/(PS-1) blends is made to zero weight fraction of PS-1, we estimate the T_{DMT} of Vector 4111 to be approximately 250 °C and the T_{LDOT} to be approximately 200 °C. Since our previous SAXS and TEM results indicate that Vector 4111 has a distorted microdomain structure at 220 °C,[43] we conclude that 200 °C cannot be regarded as being the T_{ODT} of Vector 4111.

Using SAXS, we observed that the Vector 4111/(PS-1) blends undergo first LDOT and then DMT with $T_{LDOT} < T_{DMT}$. Although the Leibler theory[55] does not distinguish the difference between LDOT and DMT, we confirmed via TEM that at $T_{LDOT} < T < T_{DMT}$ distorted microdomains were formed in each of the binary blends investigated, which have short-range spatial order, and at $T \geq T_{DMT}$ the microdomains disappeared completely. We believe that the distorted microdomain with short-range spatial order generated at $T_{LDOT} < T < T_{DMT}$ was due to the random thermal forces, which perturbed the long-range order of lamellae, hexagonally packed cylinders, or spheres in a cubic lattice that existed at temperatures just below T_{LDOT}. The presence of microdomains with short-range spatial order in a Vector 4111/(PS-1) blend was manifested by the rheological response in that Han plots having a slope of 2 in the terminal region were shifted downward with increasing temperature until reaching T_{DMT}, above which they no longer

depended on temperature. Moreover, the evidence that a higher-order shoulder exists in the SAXS profile at temperatures even above T_{LDOT}, that the asymptotic behavior of the SAXS scattering intensity distribution with respect to the magnitude of the scattering vector q is unaltered across the T_{LDOT}, and that the remarkable change in $d(\sigma_q^2)/d(1/T)$ occurs across the T_{DMT} reinforces further our conclusion that the distorted microdomains with short-range spatial order exist at $T_{LDOT} < T < T_{DMT}$. It is worth noting that the LDOT in the Vector 4111/(PS-1) blends observed by SAXS are thermally reversible. We have found that the values of T_{DMT} determined from SAXS agree very well with those determined from the Han plots.

The present study demonstrates that when investigating phase transitions in complex polymer systems such as those investigated in this study, rheological measurements alone are not sufficient. Thus, we conclude that it is imperative to combine rheological measurements with structural investigations (e.g., SAXS, TEM) to unambiguously determine phase transitions in complex polymer systems such as those investigated in this study.

References and Notes

(1) Toy, L.; Ninomi, M.; Shen, M. *J. Macromol. Sci., Phys.* **1975**, *B11*, 281.
(2) Ninomi, M.; Akovali, G.; Shen, M. *J. Macromol. Sci., Phys.* **1977**, *B13*, 133.
(3) Zin, W. C.; Roe, R. J. *Macromolecules* **1984**, *17*, 183.
(4) Hashimoto, T.; Tanaka, H.; Hasegawa, H. In *Molecular Conformation and Dynamics of Macromolecules in Condensed Systems*; Nagasawa, M., Ed.; Elsevier: Amsterdam, 1988; p 257.
(5) Kinning, D. J.; Winey, K. I.; Thomas, E. L. *Macromolecules* **1988**, *21*, 3502.
(6) Kinning, D. J.; Thomas, E. L. *J. Chem. Phys.* **1988**, *90*, 5806.
(7) Hashimoto, T.; Tanaka, T.; Hasegawa, H. *Macromolecules* **1990**, *23*, 4378.
(8) Tanaka, H.; Hasegawa, H.; Hashimoto, T. *Macromolecules* **1991**, *24*, 240.
(9) Winey, K. I.; Thomas, E. L.; Fetters, L. *J. Chem. Phys.* **1991**, *95*, 9367.
(10) Han, C. D.; Baek, D. M.; Kim, J.; Kimishima, K.; Hashimoto, T. *Macromolecules* **1992**, *25*, 3052.
(11) Hashimoto, T.; Koizumi, S.; Hasegawa, H.; Izumitani, T.; Hyde, S. T. *Macromolecules* **1992**, *25*, 1433.
(12) Winey, K. I.; Thomas, E. L.; Fetters, L. *Macromolecules* **1992**, *25*, 422.
(13) Disko, M. M.; Liang, K. S.; Beha, S. K.; Roe, R. J.; Jeon, K. J. *Macromolecules* **1993**, *26*, 2983.
(14) Kim, J. K.; Jung, D. S.; Kim, J. *Polymer* **1993**, *34*, 4613.
(15) Spontak, R. J.; Smith, S. D.; Ashraf, A. *Macromolecules* **1993**, *26*, 956, 5118.
(16) Mayes, A. M.; Russell, T. P.; Satija, S. K.; Majkrzak, C. F. *Macromolecules* **1992**, *25*, 6523.
(17) Shull, K. R.; Winey, K. I. *Macromolecules* **1992**, *25*, 2637.
(18) Koizumi, S.; Hasegawa, H.; Hashimoto, T. *Macromolecules* **1994**, *27*, 7893.
(19) Kimishima, K.; Hashimoto, T.; Han, C. D. *Macromolecules* **1995**, *28*, 3842.
(20) Roe, R. J.; Zin, W. C. *Macromolecules* **1984**, *17*, 189.
(21) Nojima, S.; Roe, R. J. *Macromolecules* **1987**, *20*, 1866.
(22) Tanaka, H.; Hashimoto, T. *Polym. Commun.* **1988**, *29*, 212.
(23) Tanaka, H.; Hashimoto, T. *Macromolecules* **1991**, *24*, 5713.
(24) Baek, D. M.; Han, C. D.; Kim, J. K. *Polymer* **1992**, *33*, 4821.
(25) Winey, K. I.; Thomas, E. L.; Fetters, L. J. *Macromolecules* **1992**, *25*, 2645.
(26) Ghijsels, A.; Raadsen, J. *Pure Appl. Chem.* **1980**, *52*, 1359.
(27) Baek, D. M.; Han, C. D. *Macromolecules* **1992**, *25*, 3706.
(28) Han, C. D.; Baek, D M.; Kim, J. K.; Chu, S. G. *Polymer* **1992**, *33*, 294.
(29) Krause, S. In *Colloidal and Morphological Behavior of Block and Graft Copolymers*; Molau, G. E., Ed.; Plenum Press: New York, 1971; p 223.
(30) Whitmore, M. D.; Noolandi, J. *Macromolecules* **1985**, *18*, 2486.
(31) Leibler, L.; Benoit, H. *Polymer* **1981**, *22*, 195.
(32) Matsen, M. W. *Macromolecules* **1995**, *28*, 5765.
(33) Janert, P. K.; Schick, M. *Macromolecules* **1998**, *31*, 1109.
(34) Han, C. D.; Vaidya, N. Y.; Kim, D.; Shin, G.; Yamaguchi, D.; Hashimoto, T. *Macromolecules* **2000**, *33*, 3767.
(35) The LDOT is subjected to a hysteresis effect. Thus, a sufficiently slow cooling process must be employed in order to clearly discern the lattice ordering process during the cooling process. It should be further noted that the rate of the lattice ordering process strongly depends on the equilibrium morphology at low temperature.
(36) Since the system is effectively small, we cannot anticipate changes in heat capacity, for instance, at T_{DMT}. However, it may be expected that if we have an experimental method that enables us to follow a single micelle with increasing temperature, the micelle would sharply disappear at and above a well-defined temperature. We think that this is DMT.
(37) The thermal stability of spheres may be larger than that of the lattice, because the free energy cost of thermal deformation of spheres can be larger than that of thermal deformation of lattices. This observation is supported by a recent experimental study,[38] which shows that the local strain imposed on spheres is much smaller than that imposed on the lattice under a large amplitude oscillatory shear at a low angular frequency.
(38) Shin, G.; Sakamoto, N.; Saijo, K.; Suehiro, S.; Hashimoto, T.; Ito, K.; Amemiya, T. *Macromolecules* **2000**, *33*, 9002.
(39) Shibayama, M.; Hashimoto, T.; Kawai, H. *Macromolecules* **1983**, *16*, 16.
(40) Hashimoto, T.; Shibayama, M.; Kawai, H.; Watanabe, H.; Kotaka, T. *Macromolecules* **1983**, *16*, 361.
(41) In refs 39 and 40, using SAXS on polymer solutions consisting of SB diblock copolymer and *n*-tetradecane, the authors reported on two transition temperatures: the lower transition temperature denoted as T_d at which an onset of line broadening of the SAXS profiles occurred due to a loss of the long-range order in the spatial arrangement of the spherical microdomains, and the higher transition temperature denoted by T_c at which the microdomain structure is dissolved into a homogeneous blend. Thus, the T_d corresponds to our T_{LDOT} and the T_c corresponds to our T_{DMT}.
(42) Most of their DM morphology was observed for the lamella-forming block copolymer blended with homopolystyrene with varying molecular weights, in contrast to our system where the DM morphology was observed for PS sphere-forming block copolymer blended with a homopolystyrene.
(43) Sakamoto, N.; Hashimoto, T.; Han, C. D.; Kim, D.; Vaidya, N. Y. *Macromolecules* **1997**, *30*, 1621.
(44) Hashimoto, T.; Suehiro, S.; Shibayama, M.; Saijo, K.; Kawai, H. *Polym. J.* **1981**, *13*, 501.
(45) Suehiro, S.; Saijo, K.; Ohta, Y.; Hashimoto, T.; Kawai, H. *Anal. Chem. Acta* **1986**, *189*, 41.
(46) Fujimura, M.; Hashimoto, T.; Kawai, H. *Mem. Fac. Eng., Kyoto Univ.* **1981**, *43*, 224.
(47) Hendricks, R. W. *J. Appl. Crystallogr.* **1972**, *5*, 315.
(48) (a) Neumann, C.; Loveday, D. R.; Abetz, V.; Stadler, R. *Macromolecules* **1998**, *31*, 2493. (b) Neumann, C.; Abetz, V.; Stadler, R. *Colloid Polym. Sci.* **1998**, *276*, 19. These authors referred to log G' vs log G'' plots as a Han plot.
(49) (a) Han, C. D.; Kim, J. *J. Polym. Sci., Polym. Phys. Ed.* **1987**, *25*, 1741. (b) Han, C. D.; Kim, J.; Kim, J. K. *Macromolecules* **1989**, *22*, 383. (c) Han, C. D.; Baek, D. M.; Kim, J. K. *Macromolecules* **1990**, *23*, 561.
(50) (a) Gouinlock, E. V.; Porter, R. S. *Polym. Eng. Sci.* **1977**, *17*, 534. (b) Chung, C. I.; Lin, M. I. *J. Polym. Sci., Polym. Phys. Ed.* **1978**, *16*, 545. (c) Widmaier, J. M.; Meyer, G. C. *J. Polym. Sci., Polym. Phys. Ed.* **1980**, *18*, 217. (d) Rosedale, J. H.; Bates, F. S. *Macromolecules* **1990**, *23*, 2329.
(51) Sakamoto, N.; Hashimoto, T.; Han, C. D.; Kim, D.; Vaidya, N. Y. *Macromolecules* **1997**, *30*, 5321.
(52) Sakamoto, N.; Hashimoto, T. *Macromolecules* **1995**, *28*, 6825.
(53) It should be noted that the behavior of this blend shown in Figures 11 and 12 looks similar to that found for the neat lamella-forming block copolymers in a previous study of Sakamoto and Hashimoto;[52,54] i.e., the T_{LDOT} determined from Figures 11 and 12 may be regarded as being equal to the conventional T_{ODT}, and the T_{DMT} determined from Figure 12 may be regarded as being equal to the mean-field (MF) to non-mean-field (non-MF) crossover temperature (T_{MF}).[52] We note that it is very difficult, if not impossible, for us to distinguish the two transitions: (i) LDOT and DMT, and (ii) ODT and MF-to-non-MF crossover for this particular 49/51 Vector 4111/(PS-1) blend using SAXS experiment alone. However, the values of T_{LDOT} and T_{DMT} determined from

Figure 12 are found to be in good agreement with those determined from an independent rheological measurement (Figure 10). Moreover, as will be seen in Figure 14, both T_{LDOT} and T_{DMT} decrease monotonically with increasing amounts of added PS-1 in all four 86/14, 73/27, 62/38, and 49/51 Vector 411/(PS-1) blends. Such a consistent trend seems to support the procedures adopted in this study to determine the T_{LDOT} and T_{DMT} of the 49/51 Vector 4111/(PS-1) blend. Note that the two transitions in the 86/14, 73/27, and 62/38 Vector 411/(PS-1) blends are well clarified as being LDOT and DMT, respectively, rather than ODT and MF-to-non-MF crossover.

(54) Sakamoto, N.; Hashimoto, T. *Macromolecules* **1998**, *31*, 3292.
(55) Leibler, L. *Macromolecules* **1980**, *13*, 1602.
(56) Bodycomb, J.; Yamaguchi, D.; Hashimoto, T. *Macromolecules* **2000**, *33*, 5187.
(57) Their observation for the systems that show lamellae and cylinders with long-range order at low temperatures is not consistent with ours, the clarification of which deserves further investigation.

MA0010682